PROCEEDINGS OF SCIENCE

Measurements of charged-particle distributions at $\sqrt{s} = 8$ and 13 TeV with the ATLAS detector

Wolfgang Lukas[*†]
University of Innsbruck
E-mail: wolfgang.lukas@cern.ch

Inclusive charged-particle measurements at hadron colliders probe the low-energy non-perturbative region of QCD. The ATLAS collaboration has measured the primary-charged-particle multiplicity and its dependence on transverse momentum and pseudorapidity in special data sets with low LHC proton–proton beam currents, recorded at centre-of-mass energies of 8 TeV and 13 TeV. The new precise measurements at 8 TeV cover a wide spectrum of distributions using charged-particle selections with minimum transverse momentum of both 100 MeV and 500 MeV and in various phase-space regions of low and high charged-particle multiplicities. Two measurements at 13 TeV present the first detailed studies with a minimum transverse momentum of 500 MeV and 100 MeV. The measurements are compared with predictions of various MC generators and are found to provide strong constraints on these.

XXIV International Workshop on Deep-Inelastic Scattering and Related Subjects
11-15 April, 2016
DESY Hamburg, Germany

[*]Speaker.
[†]On behalf of the ATLAS Collaboration.

PoS(DIS2016)199

1. Introduction

Inclusive charged-particle measurements at hadron colliders probe the non-perturbative region of soft-QCD interactions with low momentum transfer. Predictions of the hadronic final states of such processes can be made by various phenomenological models, whose parameters must be constrained by experimental data. The understanding of these strong interactions is also crucial to predict the soft-QCD background and topology of hard-scatter events with pile-up, i.e. multiple hadron collisions per bunch crossing, and to reduce systematic uncertainties of their measurements.

The ATLAS collaboration [1] has measured the primary-charged-particle multiplicity and its dependence on transverse momentum and pseudorapidity in pp collisions, using special datasets with low LHC beam currents, recorded in 2012 and 2015 at centre-of-mass energies of $\sqrt{s} = 8$ and 13 TeV [2, 3, 4]. These studies complement recent results by other LHC experiments [5, 6] and prior measurements at the LHC, Tevatron and other colliders. The new studies apply methodologies similar to those in previous ATLAS measurements at lower energies [7]; novelties are found in a more robust fiducial definition of primary charged particles, significantly reduced systematic uncertainties, and a wider scope of measurements. Four distributions of observables were measured:

$$\frac{1}{N_{\text{ev}}} \cdot \frac{\mathrm{d}N_{\text{ch}}}{\mathrm{d}\eta}, \quad \frac{1}{N_{\text{ev}}} \cdot \frac{1}{2\pi p_{\text{T}}} \cdot \frac{\mathrm{d}^2 N_{\text{ch}}}{\mathrm{d}\eta\, \mathrm{d}p_{\text{T}}}, \quad \frac{1}{N_{\text{ev}}} \cdot \frac{\mathrm{d}N_{\text{ev}}}{\mathrm{d}n_{\text{ch}}} \quad \text{and} \quad \langle p_{\text{T}} \rangle \text{ versus } n_{\text{ch}}.$$

Here n_{ch} is the number of primary charged particles (with mean lifetime $\tau > 300\,\text{ps}$ and originating directly from pp interactions or from decays of short-lived particles with $\tau < 30\,\text{ps}$) in an event, η denotes a particle's pseudorapidity, p_{T} is the transverse momentum component of the charged particle relative to the beam direction, N_{ev} is the total number of events corresponding to a given selection, and N_{ch} is the total number of primary charged particles in all selected events.

Final results are given for phase spaces defined by kinematic selections of particles with $|\eta| < 2.5$ and either ($p_{\text{T}} > 100$ MeV, $n_{\text{ch}} \geq 2$) or ($p_{\text{T}} > 500$ MeV, $n_{\text{ch}} \geq 1$). The 8 TeV measurement also gives results for higher-multiplicity events ($p_{\text{T}} > 500$ MeV, $n_{\text{ch}} \geq 6, 20$ and 50) of which the latter two event types have hitherto not been measured by ATLAS. The 13 TeV study at $p_{\text{T}} > 500$ MeV also provides measurements for $|\eta| < 0.8$ to facilitate comparison with other LHC experiments.

The presented studies use tracks that are reconstructed from charged particles measured with the inner tracker (ID) of ATLAS [1]. The ID is embedded within a 2 T axial magnetic field provided by a solenoid, has full coverage in ϕ and covers the pseudorapidity range $|\eta| < 2.5$. It comprises a silicon pixel detector (Pixel), a silicon microstrip detector (SCT) and a transition radiation tracker (TRT), organised into barrel and end-cap parts. In the 8 TeV (13 TeV) study, the barrel consists of three (four) Pixel layers, four SCT double-layers of microstrips with a 40 mrad stereo angle, and 73 layers of TRT straw tubes. A new fourth innermost pixel barrel layer with high granularity, called Insertable B-Layer (IBL), which aids the track reconstruction and improves resolutions of track parameters, has been installed prior to the 13 TeV studies. The data were recorded based on signals from the minimum-bias trigger scintillators (MBTS), installed in front of the end-cap calorimeter cryostats at $z = \pm 3.56\,\text{m}$ and covering the range $2.08\ (2.07) < |\eta| < 3.75\ (3.86)$ at 8 TeV (13 TeV).

2. Monte Carlo simulation and data selection

Monte Carlo (MC) models of inclusive pp interactions, with parameter settings (tunes) opti-

mised to reproduce existing data, were used to generate event samples. PYTHIA 8 [8] employs the A2 [9] and MONASH [10] tunes with the MSTW2008LO and NNPDF2.3LO parton distribution functions (PDF), respectively. EPOS [11] uses the LHC tune [12], while QGSJET-II [13] employs the default settings. The generated events were processed by the ATLAS simulation framework [14] based on GEANT4 [15] to simulate the detector response, accounting for inactive and inefficient regions. The resulting datasets were used to derive corrections for detector effects and to evaluate systematic uncertainties. The generated hadronic final states were compared to the corrected data.

The data were recorded in special runs with a low average number of inelastic pp interactions per bunch crossing, $\langle\mu\rangle < 0.01$. These datasets correspond to integrated luminosities of $160\,\mu\text{b}^{-1}$ [2], $170\,\mu\text{b}^{-1}$ [3] and $151\,\mu\text{b}^{-1}$ [4]. In each analysis, ≈ 9 million events were selected from colliding bunches with at least one MBTS signal above threshold. A reconstructed primary vertex [16] was required with at least two associated tracks possessing $p_\text{T} > 100$ MeV, constrained to the luminous z-region of the measured beam position. Events with an additional vertex with ≥ 4 associated tracks were rejected, thus reducing pile-up events to a negligible level of $< 0.01\,\%$.

Tracks were reconstructed in the silicon detectors and extended into the TRT using a special configuration of two pattern recognition algorithms [17]. Tracks were required to have $|\eta| < 2.5$ and $p_\text{T} > 100$ MeV, at least one pixel measurement (hit), a hit in the innermost pixel layer if the extrapolated track passed through an active region in that layer (in 13 TeV studies, if the track passed through an inactive IBL region, this criterion is applied to the next pixel layer), and at least 2, 4 or 6 SCT hits depending on the transverse momentum of the track. Poorly measured high-p_T tracks above 10 GeV were suppressed by requiring a track fit χ^2 probability of > 0.01. The distance of closest approach in the transverse ($|d_0|$) and longitudinal plane ($|z_0 \cdot \sin\theta|$) with respect to the primary vertex (8 TeV) or beam line (13 TeV) was required to be $< 1.5\,\text{mm}$. Distributions of average numbers of hits per track in data and MC simulation are presented in Figures 1a and 1b.

3. Correction procedure and systematic uncertainties

Inclusive final-state distributions were obtained by applying event- and track-level weights to compensate for selection and reconstruction inefficiencies and for background contaminations. The event weight, parameterised by the track multiplicity, compensates for lost events due to inefficiencies of the MBTS trigger selection and the vertex reconstruction algorithm. The track weight was estimated for each track as a function of p_T and η, based on the track reconstruction efficiency, the fraction of non-primary tracks, the fraction of tracks associated with strange baryons, and the fraction of tracks migrating into the kinematic region due to resolution effects.

The track reconstruction efficiency was determined from MC simulation and parameterised by p_T and η. It is defined as the fraction of generated primary charged particles which are uniquely associated (matched) to reconstructed tracks, based on their smallest angular distance (8 TeV) or the track hit matching probability (13 TeV). It is strongly affected by the amount of material traversed by charged particles, which increases the probability of particle–matter interactions. This is the dominating source of systematic uncertainties in most regions of the measured distributions, resulting mainly from the uncertainty of the detector material description used in the simulation. Owing to extensive studies of material interactions [18, 19] the amount of material within the ID was constrained to $\pm 5\,\%$, leading to a significant reduction of the systematic uncertainty with re-

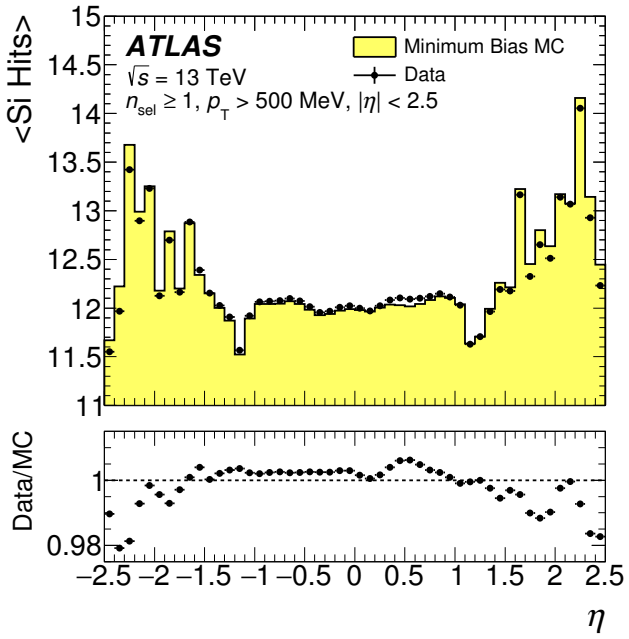

(a)

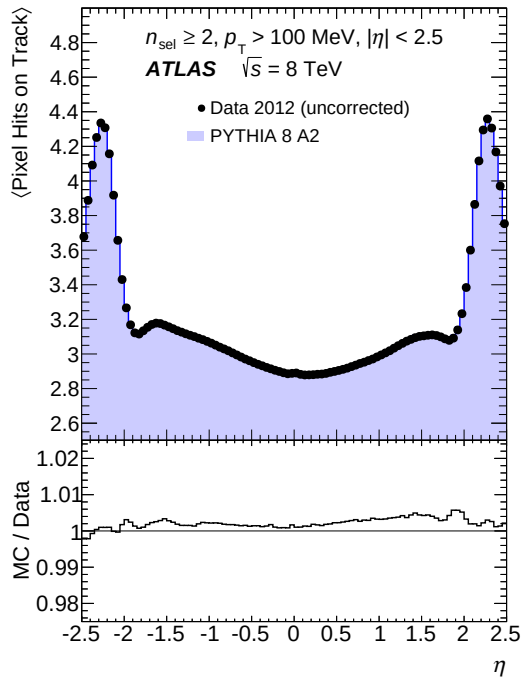

(b)

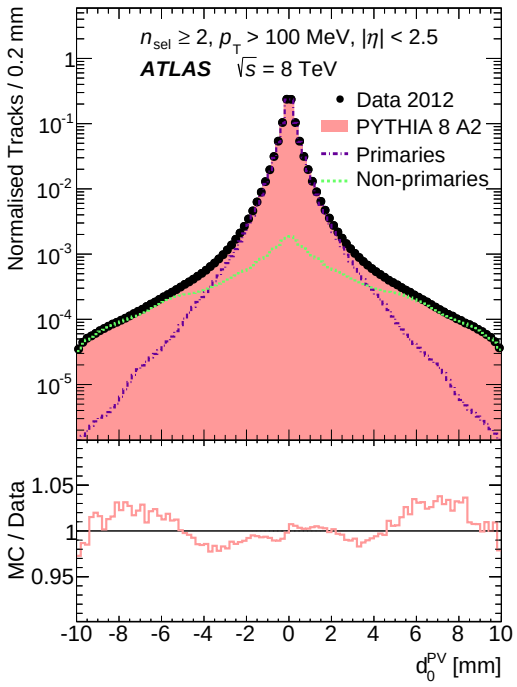

(c)

Figure 1: Data and MC simulation of the average number of hits per reconstructed track as a function of pseudorapidity, η, in (a) the pixel and SCT detectors at $\sqrt{s} = 13$ TeV for $p_{\mathrm{T}} > 500$ MeV tracks and (b) the pixel detector at $\sqrt{s} = 8$ TeV for $p_{\mathrm{T}} > 100$ MeV tracks. (c) Normalised transverse impact parameter distributions of reconstructed tracks with $p_{\mathrm{T}} > 100$ MeV in data and MC simulation at 8 TeV; the MC distributions have been reweighted to match the reconstructed p_{T} spectrum in data. Plots are taken from Refs. [2] and [3].

spect to earlier measurements. In the 13 TeV studies the IBL material was constrained to $\pm 10\,\%$, and differences between data and simulation at $|\eta| > 1.5$ due to new pixel services were accounted for by estimating the effect of +50 % material in this region [4] or by a data-driven correction [3].

The fraction of charged non-primary particles, originating mostly from hadronic interactions, photon conversions and weak decays, was estimated by fitting shapes of the d_0 distributions in MC simulations to the data in various p_{T} intervals, and was subtracted. A fitted inclusive d_0 distribution is shown in Figure 1c. Contributions from fake tracks and non-collision background (beam–gas interactions, scattering from up-stream collimators, and cosmic rays) were found to be negligible.

A novel aspect of the presented studies is that a primary charged particle is now defined as having a mean lifetime $\tau > 300\,\mathrm{ps}$, instead of the previously used definition $\tau > 30\,\mathrm{ps}$. Charged particles with $30 < \tau < 300\,\mathrm{ps}$ (strange baryons) are excluded due to their low reconstruction efficiency to minimise model dependences in the correction procedure; the p_{T}-dependent fraction of tracks associated with them was estimated from the EPOS LHC simulation and subtracted. Decay products of all particles with $\tau > 30\,\mathrm{ps}$ are considered as secondary particles and excluded.

An iterative Bayesian unfolding procedure [20] was applied to the corrected n_{ch} and p_{T} distributions, and to $\langle p_{\mathrm{T}} \rangle$ versus n_{ch}, to compensate for migration and resolution effects between the observed and true values. The unfolded n_{ch} distribution was also corrected to account for events migrating out of the multiplicity range required by the phase space. The total number of events N_{ev}, obtained by integrating the n_{ch} distribution, was used to normalise the p_{T}, η and n_{ch} distributions.

Individual sources of systematic uncertainty were applied separately as variations of the event or track weights, or by varying the input distributions or unfolding matrices which were used for the Bayesian unfolding procedure, thus producing alternative versions of the final results. The differences from the nominal results were taken as systematic uncertainties and added in quadrature. The dominant sources of systematic uncertainty were due to incomplete knowledge of the material distribution in the ID and due to uncertainties associated with the unfolding technique.

4. Results

Distributions of primary charged particles at 8 and 13 TeV are given in Figures 2a to 2d for the most inclusive phase space defined by $n_{\mathrm{ch}} \geq 2$ and $p_{\mathrm{T}} > 100$ MeV. Similar results are obtained across all three studies and all measured phase spaces. The EPOS LHC tune models the p_{T} spectra well and gives a fair description of the n_{ch} spectra, followed by PYTHIA 8 calculations which underestimate the event yield at low and high n_{ch}. In the $\langle p_{\mathrm{T}} \rangle$ versus n_{ch} distribution the EPOS and PYTHIA 8 models, which implement colour coherence effects, provide fair descriptions of the data. In all distributions (except pseudorapidity) QGSJET-II shows large disagreements with the data.

The evolution of the primary-charged-particle multiplicity per unit pseudorapidity at $\eta = 0$, computed by averaging over $|\eta| < 0.2$, is shown in Figure 3, with values given in Table 1. For consistent comparisons with previous measurements, the new results were corrected to the earlier definition of stable particles, using extrapolation factors derived from EPOS LHC predictions with uncertainties following comparisons of different MC models. Owing to the improved knowledge of the ID material [18, 19], the total uncertainty in the new measurements [2, 3, 4] is about 30–40 % less than in previous studies [7]. The best description of the multiplicity evolution with centre-of-mass energy is given by the EPOS LHC model, followed by the PYTHIA 8 tunes.

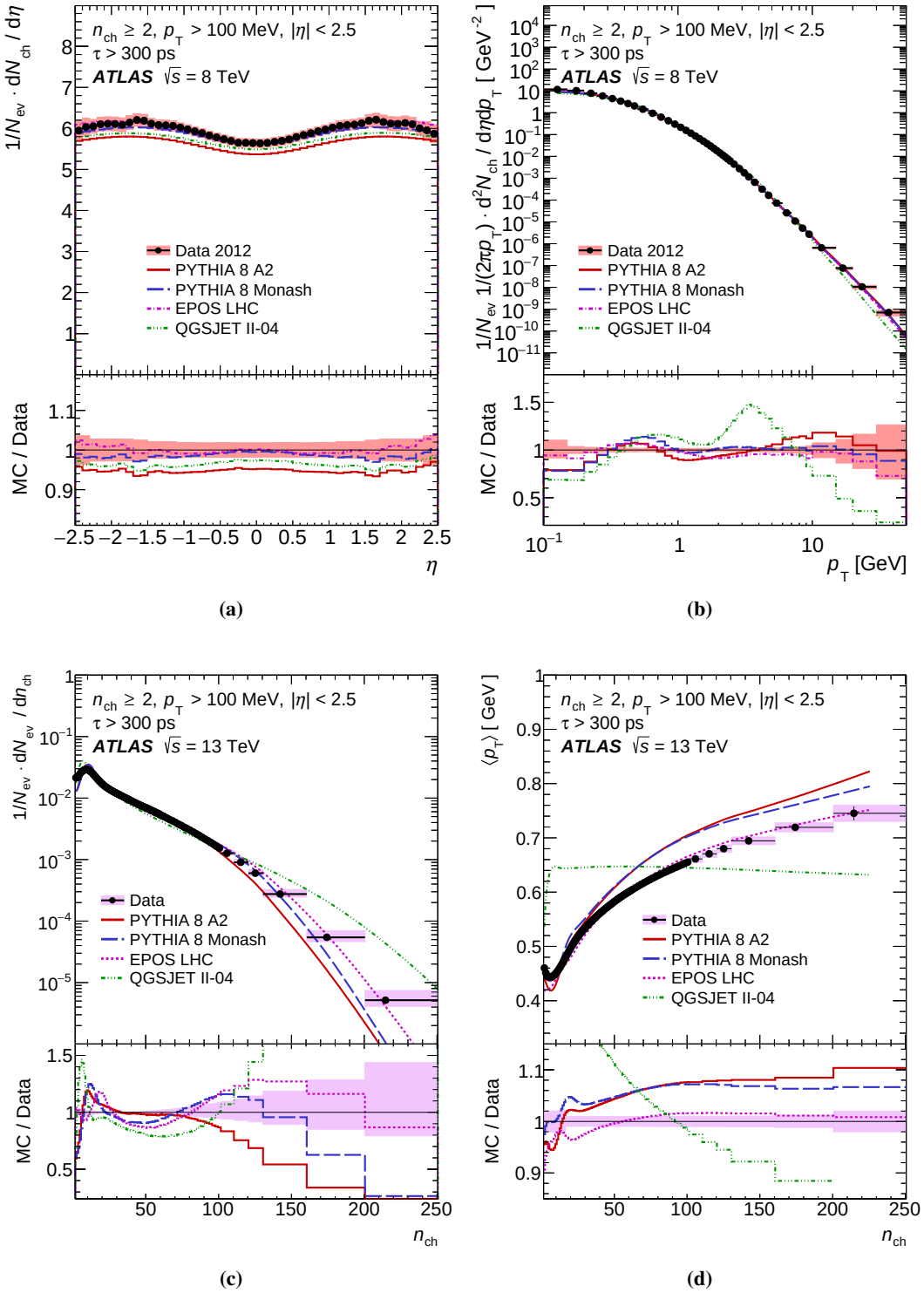

Figure 2: Distributions of primary charged particles at $\sqrt{s} = 8$ and 13 TeV for events with $n_{ch} \geq 2$, $p_T > 100$ MeV and $|\eta| < 2.5$ as a function of (a) pseudorapidity, η, (b) transverse momentum, p_T, (c) multiplicity, n_{ch}, and (d) average transverse momentum, $\langle p_T \rangle$, versus multiplicity. The data, represented by full markers, are compared to various final-state MC predictions, which are shown by curves. The shaded areas and error bars around the data points represent the total statistical and systematic uncertainties added in quadrature. Plots are taken from Refs. [2] and [4].

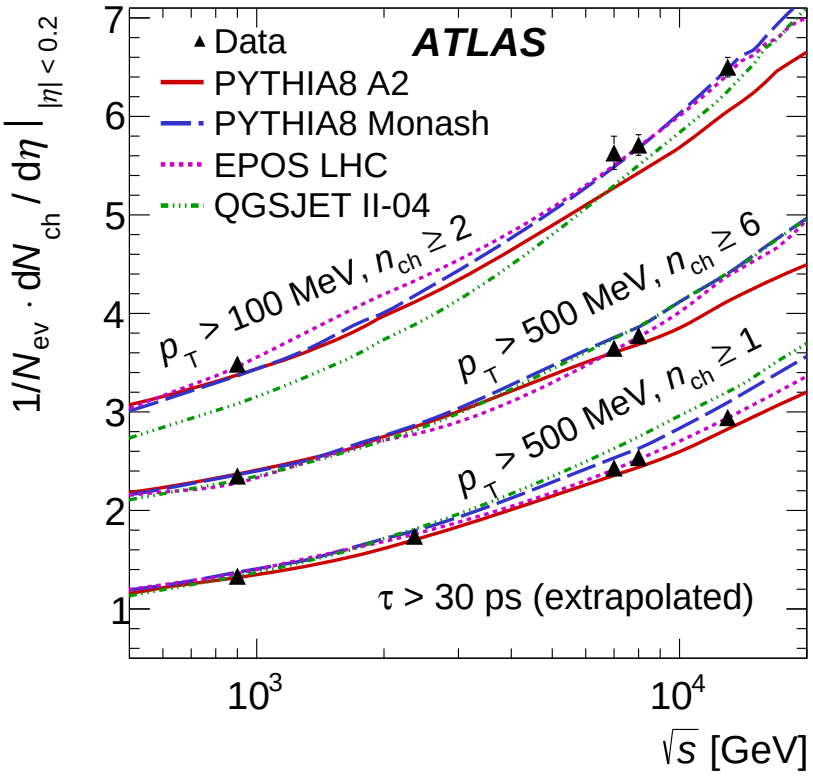

Figure 3: Central primary-charged-particle multiplicity per unit of pseudorapidity at $|\eta| < 0.2$ as a function of the centre-of-mass energy, shown for three phase spaces; the new results at $\sqrt{s} = 8$ and 13 TeV are extrapolated to include strange baryons. The data, represented by full markers, are compared to various final-state MC predictions, which are shown by curves. The shaded areas and error bars around the data points represent the total statistical and systematic uncertainties added in quadrature. Plots are taken from Ref. [4].

5. Conclusion

Measurements of distributions of primary charged particles produced in minimum-bias pp collisions at $\sqrt{s} = 8$ and 13 TeV with the ATLAS detector at the LHC are presented. The central primary-charged-particle multiplicities at $|\eta| < 0.2$ per event and unit of pseudorapidity are determined with the previously used as well as a new fiducial definition, yielding total uncertainties that are 30–40 % smaller than for the previous highest precision ATLAS measurements. The 8 TeV study also presents new measurements of final states at high multiplicities of $n_{ch} \geq 20$ and $n_{ch} \geq 50$, while the 13 TeV studies provide first measurements with the updated ATLAS geometry and the new IBL, including a restricted phase space to facilitate comparisons with other LHC experiments. Predictions of various MC models were compared with the data, and the best description was found to be given by the EPOS LHC tune, followed by the PYTHIA 8 A2 and MONASH tunes. These results provide valuable constraints for the tuning and further understanding of soft-QCD models.

Energy	**Phase Space**		$1/N_{\text{ev}} \cdot \mathrm{d}N_{\text{ch}}/\mathrm{d}\eta$ **at** $\lvert\eta\rvert < 0.2$	
$\sqrt{s}$	$n_{\text{ch}} \geq$	$p_{\text{T}} >$	$\tau > 300\,\text{ps}$ (fiducial)	$\tau > 30\,\text{ps}$ (extrapolated)
8 TeV	2	100 MeV	5.64 $\pm$ 0.10	5.71 $\pm$ 0.11
8 TeV	1	500 MeV	2.477 $\pm$ 0.031	2.54 $\pm$ 0.04
8 TeV	6	500 MeV	3.68 $\pm$ 0.04	3.78 $\pm$ 0.05
8 TeV	20	500 MeV	6.50 $\pm$ 0.05	6.66 $\pm$ 0.07
8 TeV	50	500 MeV	12.40 $\pm$ 0.15	12.71 $\pm$ 0.18
13 TeV	2	100 MeV	6.42 $\pm$ 0.10	6.50 $\pm$ 0.10
13 TeV	1	500 MeV	2.874 $\pm$ 0.033	2.94 $\pm$ 0.04

Table 1: Central primary-charged-particle density $1/N_{\text{ev}} \cdot \mathrm{d}N_{\text{ch}}/\mathrm{d}\eta$ at $\lvert\eta\rvert < 0.2$ for five phase spaces. Results are given for the fiducial definition $\tau > 300\,\text{ps}$, and for the previously used definition $\tau > 30\,\text{ps}$ using extrapolation factors to account for the fraction of charged strange baryons predicted by EPOS LHC simulation.

References

[1] ATLAS Collaboration, *The ATLAS Experiment at the CERN Large Hadron Collider*, JINST **3** (2008) S08003.

[2] ATLAS Collaboration, *Charged-particle distributions in pp interactions at $\sqrt{s} = 8$ TeV measured with the ATLAS detector*, Eur. Phys. J. C **76** (2016) 403 [hep-ex/1603.02439].

[3] ATLAS Collaboration, *Charged-particle distributions in $\sqrt{s} = 13$ TeV pp interactions measured with the ATLAS detector at the LHC*, Phys. Lett. B **758** (2016) 67–88 [hep-ex/1602.01633].

[4] ATLAS Collaboration, *Charged-particle distributions at low transverse momentum in $\sqrt{s} = 13$ TeV pp interactions measured with the ATLAS detector at the LHC*, Eur. Phys. J. C **76** (2016) 502 [hep-ex/1606.01133].

[5] CMS Collaboration, *Pseudorapidity distribution of charged hadrons in proton–proton collisions at $\sqrt{s} = 13$ TeV*, Phys. Lett. B **751** (2015) 143–163 [hep-ex/1507.05915].

[6] ALICE Collaboration, *Pseudorapidity and transverse-momentum distributions of charged particles in proton–proton collisions at $\sqrt{s} = 13$ TeV*, Phys. Lett. B **753** (2016) 319–329 [nucl-ex/1509.08734].

[7] ATLAS Collaboration, *Charged-particle multiplicities in pp interactions measured with the ATLAS detector at the LHC*, New J. Phys. **13** (2011) 053033 [hep-ex/1012.5104].

[8] T. Sjöstrand, S. Mrenna and P. Z. Skands, *A Brief Introduction to PYTHIA 8.1*, Comp. Phys. Comm. **178** (2008) 852–867 [hep-ph/0710.3820].

[9] ATLAS Collaboration, *Further ATLAS tunes of PYTHIA6 and Pythia 8*, ATL-PHYS-PUB-2011-014 (2011).

[10] P. Skands, S. Carrazza and J. Rojo, *Tuning PYTHIA 8.1: the Monash 2013 Tune*, Eur. Phys. J. C **74** (2014) 3024 [hep-ph/1404.5630].

[11] S. Porteboeuf, T. Pierog and K. Werner, *Producing Hard Processes Regarding the Complete Event: The EPOS Event Generator*, in proceedings of *45th Rencontres de Moriond* (2010) [hep-ph/1006.2967].

[12] T. Pierog, Iu. Karpenko, J. Katzy, E. Yatsenko and K. Werner, *EPOS LHC: Test of collective hadronization with data measured at the CERN Large Hadron Collider*, Phys. Rev. C **92** (2015) 034906 [hep-ph/1306.0121].

[13] S. Ostapchenko, *Monte Carlo treatment of hadronic interactions in enhanced Pomeron scheme: I. QGSJET-II model*, Phys. Rev. D **83** (2011) 014018 [hep-ph/1010.1869].

[14] ATLAS Collaboration, *The ATLAS Simulation Infrastructure*, Eur. Phys. J. C **70** (2010) 823–874, [physics.ins-det/1005.4568].

[15] GEANT4 Collaboration, S. Agostinelli et al., *GEANT4: A Simulation toolkit*, Nucl. Instrum. Meth. A **506** (2003) 250–303.

[16] ATLAS Collaboration, *Performance of primary vertex reconstruction in proton–proton collisions at* $\sqrt{s} = 7$ *TeV in the ATLAS experiment*, ATLAS-CONF-2010-069 (2010).

[17] T. Cornelissen et al., *The new ATLAS track reconstruction (NEWT)*, JPCS **119** (2008) 032014.

[18] W. Lukas, *ATLAS inner tracking detectors: Run 1 performance and developments for Run 2*, Nucl. Part. Phys. Proc. **273–275** (2016) 1134–1140.

[19] ATLAS Collaboration, *Studies of the ATLAS Inner Detector material using* $\sqrt{s} = 13$ *TeV pp collision data*, ATL-PHYS-PUB-2015-050 (2015).

[20] G. D'Agostini, *A Multidimensional unfolding method based on Bayes' theorem*, Nucl. Instrum. Meth. A **362** (1995) 487–498.